

Generalizations of "universal dielectric response" and a general distribution-of-activation-energies model for dielectric and conducting systems

J. Ross Macdonald

Department of Physics and Astronomy, University of North Carolina, Chapel Hill, North Carolina 27514

(Received 12 November 1984; accepted for publication 15 May 1985)

Three empirical equations introduced by Jonscher to represent the imaginary part of the small-signal frequency response of dielectric materials and termed "universal dielectric response" by him are generalized in three ways. The equations may be applied in normalized form at the impedance level as well as at the usual complex dielectric constant level, defining the response of conducting rather than dielectric materials. They are generalized to include real as well as imaginary parts where possible. A unified dielectric or conductive distribution-of-activation-energies (DAE) physical model is proposed whose predictions agree remarkably well with those of all the Jonscher universal dielectric response equations as well as with many other common dielectric response equations. The new model, unlike previous small-signal response models, leads to quantitative predictions for the temperature dependence of the power-law frequency exponent appearing in the ubiquitous constant-phase-response frequency region of the total response.

INTRODUCTION

The measurement of the small-signal ac frequency response of materials over a wide range of frequencies, i.e., impedance spectroscopy (IS), is becoming a valuable analysis and characterization tool with the advent of automatic data gathering equipment. Measurements alone are usually not enough, however. Much more can be learned when measurements are interpreted using appropriate models and equations. Here I shall discuss a class of empirical equations which have proved useful for such analysis and relate them to a plausible physically realistic model. Some time ago Jonscher independently introduced¹ the constant-phase-element (CPE) small-signal ac response function of Fricke² and Cole and Cole³ and characterized it as "universal dielectric response" (UDR). At the admittance level, full CPE response may be written with two different parametrizations,⁴ as

$$Y_{CPE} = A_0(i\omega)^n = A_1(i\omega\tau_c)^n. \quad (1)$$

Here $\omega \equiv 2\pi\nu$ is the angular frequency; A_0 and A_1 are frequency-independent parameters; and $0 \leq n \leq 1$, although Jonscher has usually required $0 < n < 1$.

Jonscher and his co-workers have done a thorough job of collecting together a large amount of small-signal ac data, primarily for dielectric materials, and have shown that the complex dielectric constant, $\epsilon \equiv \epsilon' - i\epsilon''$, often exhibits one or more regions of power-law frequency response, such as that of Eq. (1). Such conclusions have led Jonscher to propose two further empirical response laws.^{1,5-8} In terms of the complex dielectric susceptibility $\chi \equiv (\epsilon - \epsilon_\infty)/\epsilon_0 \equiv \chi' - i\chi''$, the three expressions which have come to be included under the rubric of UDR are

$$\chi'' = K_0\omega^{n-1}, \quad (2)$$

$$\chi'' = K_1[(\omega/\omega_c)^{n_1-1} + (\omega/\omega_c)^{n_2-1}], \quad (3)$$

and

$$\chi'' = K_2[(\omega/\omega_p)^{-m} + (\omega/\omega_p)^{1-n}]^{-1}, \quad (4)$$

where the K_i 's are constants which are sometimes taken equal to one; the exponents fall in the range (0,1); ω_p is a peak frequency; and Eq. (2) is an immediate consequence of Eq. (1). Note that when $K_1 = 1$ in Eq. (3) or $K_2 = 1$ in Eq. (4), one obtains the too-special results, $\chi'' = 1$ or $\chi'' = 0.5$, respectively, when $\omega = \omega_c$ or $\omega = \omega_p$. Equation (3) is just a direct combination of two Eq. (2) terms. In the definition of χ , ϵ_0 and ϵ_∞ are limiting low- and high-frequency values of ϵ .

If one finds that measurements on a specific material lead to response like that of one of the above equations for a particular frequency range, it must not be assumed that such response continues to arbitrarily low or high frequencies. For example, the distribution of relaxation times function corresponding to the Eq. (1) response taken over all frequencies is non-normalizable,⁹ and Eqs. (2)-(4) all readily lead to conductivities surpassing that of copper at sufficiently high frequencies. A given relaxation process in a real system (and realistic models of it) will have a smallest and a largest response time,¹⁰ say τ_0 and τ_∞ , leading^{1,11,12} to the requirement that χ'' of a single, not composite, system be proportional to ω for $\omega < \tau_\infty^{-1}$ and to ω^{-1} for $\omega > \tau_0^{-1}$. See, however, the discussion for a composite system in the next section. These requirements are automatically satisfied for single-time-constant simple Debye response but are clearly not satisfied for UDR. Nevertheless, a great deal of small-signal data exhibit much broader $\chi''(\omega)$ curves than that of Debye, and equations and models which can be used to fit and interpret such broad-spectrum data are needed. Although the present UDR empirical equations are useful over limited-frequency ranges, a physically realistic model which could approximate UDR response in some ranges but which did not require modifications at frequency extremes would be preferable. Such a model and some of its predictions are discussed later in this work.

EXTENSION TO NEW SYSTEMS

The first generalization we present follows when a system duality relation¹² is applied to the UDR results. It can be best demonstrated by initially writing the UDR relations in standard dimensionless form as follows. Define $U_i \equiv U'_i + U''_i$ as a particular immittance function, such as a complex dielectric constant, $\epsilon = \epsilon' - i\epsilon'' \equiv \epsilon' + i\epsilon''_n$, or impedance, $Z = Z' + iZ''$, and let

$$I_i \equiv (U_i - U_{i\infty}) / (U_{i0} - U_{i\infty}) \equiv I'_i + iI''_i, \quad (5)$$

where U_{i0} and $U_{i\infty}$ are the $\omega \rightarrow 0$ and $\omega \rightarrow \infty$ limits of U'_i . When $i = \epsilon$, $U_\epsilon = \epsilon$, and when $i = Z$, $U_Z = Z$. We have introduced $\epsilon''_n \equiv -\epsilon''$ here so that U''_i has the same sign for both $i = \epsilon$ and $i = Z$. It should be understood that when several processes are present but the one of interest is concentrated in a given, possibly wide, frequency region, the U_{i0} and $U_{i\infty}$ limits merely prescribe frequencies where the process of interest has led to response much smaller than any surrounding response from other processes. With the above normalization, as $\omega \rightarrow 0$ $I'_i \rightarrow 1$, and as $\omega \rightarrow \infty$ $I'_i \rightarrow 0$. There is a problem, however, with processes such as those that lead to the CPE since for them Z' or ϵ' approach infinity as $\omega \rightarrow 0$, precluding the use of an U_{i0} associated with the process in question in the normalization. When such response is present, we will, when practical, define U_{i0} exclusive of such response, allowing Eq. (5) to still apply. Otherwise, we shall take $I_i = U_i$ in such cases as a nontransformed representation of U_i . The problem arises because no physically realizable model leads to CPE response over all frequencies, but it is still convenient to use the CPE form of Eq. (1) for comparisons with other response equations.

Now the duality relation specifies that any small-signal ac response function normalized as above may be employed at either the complex dielectric constant level or at the impedance level, no matter at which level it was originally taken to apply. We may therefore rewrite Eqs. (2)–(4) in terms of the general I_i function defined in Eq. (5), obtaining

$$I''_i = -B_{i0} \omega^{-\psi_i}, \quad (6)$$

$$I'_i = -B_{i1} \left[(\omega/\omega_{ic})^{-\psi_{i1}} + (\omega/\omega_{ic})^{-\psi_{i2}} \right], \quad (7)$$

and

$$I'_i = -B_{i2} \left[(\omega/\omega_{ip})^{-\psi_{i3}} + (\omega/\omega_{ip})^{\psi_{i4}} \right]^{-1}, \quad (8)$$

where the B 's are frequency-independent quantities. These results now apply at either the ϵ or Z levels, but the ψ_i power-law exponents and other parameters need not be the same at the two levels. For convenience let $\tau_{ic} \equiv \omega_{ic}^{-1}$ and $\tau_{ip} \equiv \omega_{ip}^{-1}$.

The possible range of all the general ψ_i exponents is (0,1). For $i = \epsilon$, we may take the UDR definitions, $\psi_\epsilon = 1 - n$, $\psi_{\epsilon 1} = 1 - n_1$, $\psi_{\epsilon 2} = 1 - n_2$, $\psi_{\epsilon 3} = m$, and $\psi_{\epsilon 4} = 1 - n$. Equations (6) and (7) yield the same exponents when they are transformed to the admittance level for both the $i = \epsilon$ and the $i \equiv Z$ choices in frequency regions where a single term dominates if we further choose $\psi_Z = n$, $\psi_{Z 1} = n_1$, and $\psi_{Z 2} = n_2$. Note especially that a parallel combination of terms, as in Eq. (7) for $i = \epsilon$, translates to a series combination for the corresponding $i = Z$ system. These results make the UDR forms, originally applied only at the ϵ level, available to describe systems at the Z level. One

should not always expect to find general I''_i response proportional to ω as $\omega \rightarrow 0$. Consider a composite system rather than an ideal single process $i = Z$ or $i = \epsilon$ system. A composite system which includes at the ϵ level a nonconducting dielectric model with an ideal resistor in parallel or at the impedance level a conducting model with an ideal capacitor in series both exhibit ω^{-1} response for I''_i in the $\omega \rightarrow 0$ limit.

EXTENSION TO COMPLETE COMPLEX FUNCTIONS

Fitting of complex data to a model is best carried out when not just the imaginary part of a function is used over a given frequency range but when the full immittance function of the model is available and is employed in the fit using complex nonlinear least-squares fitting¹³ (CNLS). The immediate generalization of Eqs. (2) and (6) to the complex regime is just the usual CPE,⁴ written in the I_i form as

$$I_i = C_{i0} (i\omega)^{-\psi_i} = (i\omega\tau_{ic})^{-\psi_i}, \quad (9)$$

where the second form is less general than the first. This result could be termed the first generalized Jonscher equation, GJ1, but even the $i = \epsilon$ form of it predates Jonscher's work. The natural extension of Eq. (7) to full immittance rank is clearly

$$I_i = C_{i1} (i\omega)^{-\psi_{i1}} + C_{i2} (i\omega)^{-\psi_{i2}},$$

or

$$I_i = B_{i1} \left[(i\omega\tau_{i1})^{-\psi_{i1}} + (i\omega\tau_{i2})^{-\psi_{i2}} \right]. \quad (10)$$

In order for the I''_i of the second form of Eq. (10) to agree with that of Eq. (7) we must take

$$\tau_{i1} \equiv \tau_{ic} \left[\sin(\pi\psi_{i1}/2) \right]^{\psi_{i1}}, \quad (11)$$

and

$$\tau_{i2} \equiv \tau_{ic} \left[\sin(\pi\psi_{i2}/2) \right]^{\psi_{i2}}. \quad (12)$$

The above choices of τ_{i1} and τ_{i2} , mandated by the original UDR form, preclude ψ_{i1} and ψ_{i2} from reaching zero. For convenient future reference, let us define Eq. (10) with the above specific τ_{i1} and τ_{i2} values as the generalized second Jonscher equation, the GJ2. It should be pointed out that since Eqs. (9) and (10) lead to $|I_i| \rightarrow \infty$ as $\omega \rightarrow 0$, their use over the full frequency range leads to unacceptable infinite values of ϵ_0 and R_0 . The problem can be avoided by applying them only for frequencies not too close to zero and defining ϵ_0 and/or R_0 independent of the processes which lead to these equations. The new model discussed later avoids these difficulties since it yields proper $\omega^{\pm 1}$ behavior at the frequency extremes.

The generalization of Eq. (3) represented by the first form of Eq. (10), with $i = \epsilon$ only, has been proposed recently by Almond and West,¹⁴ although they did not identify their expression as involving CPE's. Unfortunately, these authors elected to write each separate CPE term in the form (when we transform from their admittance expression to I_ϵ),

$$I_\epsilon = D_\epsilon \omega^{-\psi_\epsilon} \left[1 - i \tan(\pi\psi_\epsilon/2) \right] \quad (13)$$

instead of the more appropriate form⁴ which follows directly from Eq. (9),

$$I_{\epsilon\text{CPE}} = C_\epsilon \omega^{-\psi_\epsilon} \left[\cos(\pi\psi_\epsilon/2) - i \sin(\pi\psi_\epsilon/2) \right], \quad (14)$$

which does not lead to an infinite result for I''_ϵ as $\psi_\epsilon \rightarrow 1$. The Almond and West results for $i = \epsilon$ involve just two CPE's in parallel. When $i = Z$, on the other hand, the CPE's are in series, a situation explored without the use of complex non-linear least-squares data fitting¹³ by Jonscher and Réau¹⁵ and with such fitting of real and imaginary data simultaneously by Macdonald and Cook.¹⁶

Another response equation which can be related^{17,18} to Eqs. (3) and (10) is

$$I_i = [1 + (i\omega\tau_{ic})^{\psi_i}]^{-1}. \quad (15)$$

If we again take $\psi_Z = n$ and $\psi_\epsilon = 1 - n$, I_Z becomes just the empirical equation proposed quite some time ago by Ravine and Souquet¹⁹ to represent symmetrical arcs whose centers may be below the real axis, a situation often found when impedance data on conducting systems are plotted in the complex plane. The above choice makes I_ϵ just the well-known dielectric response function of Cole and Cole.³ It therefore seems reasonable to designate the general I_i function of Eq. (15), which unifies these approaches, as the ZC response function. Like the UDR equations, the ZC fails to lead to $\omega^{\pm 1}$ behavior at the frequency extremes, although its distribution of relaxation times function is normalizable. The general ZC expression of Eq. (15) leads for $i = Z$ to a circuit made up of the (ZC)_Z element, i.e., $(R_0 - R_\infty)$ times the I_Z expression of Eq. (15), in series with R_∞ . Alternatively, for $i = \epsilon$, the appropriate circuit is a (ZC)_ε element, $(C_0 - C_\infty)$ times the I_ϵ expression of Eq. (15), in parallel with the limiting capacitance C_∞ . But the ZC elements themselves may be considered either as unitary circuit components in their own right, possibly involving a distribution of relaxation times,^{3,9} or as a combination of an ideal circuit and a CPE.⁴ For $i = Z$, the combination of a resistance $(R_0 - R_\infty)$ in parallel with a CPE impedance leads to (ZC)_Z, while for $i = \epsilon$ the capacitance $(C_0 - C_\infty)$ in series with a CPE leads to (ZC)_ε.

It is not in general possible to give a closed-form immitance expression whose imaginary part corresponds exactly to the general I''_i of Eq. (8) and which leads to the Jonscher form (4). Thus no complete function like the ZC is available for use in complex least-squares fitting of data. It is possible, however, to obtain expressions for I'_i and thus I_i in certain special cases. When $\psi_{i3} = \psi_{i4} \equiv \psi_i$, I'_i is symmetrical, reducing to the form first proposed by Fuoss and Kirkwood,²⁰ an expression found to fit many symmetrical data curves quite well. An equation for the corresponding I'_i function for any fractional value of ψ_i of the form (odd integer/arbitrary integer) is available,²¹ as well as a result²² for any values of ψ_{i3} and ψ_{i4} satisfying $\psi_{i3} + \psi_{i4} = 1$. The results of the different approaches agree for $\psi_{i3} = \psi_{i4} \equiv \psi_i = 0.5$ where they overlap. In general, when $\psi_{i3} = \psi_{i4} \equiv \psi_i$, one finds²¹ that the B_{i2} factor of Eq. (8) becomes just ψ_i . The result may be written

$$I''_i = -\psi_i / [(\omega/\omega_{ip})^{-\psi_i} + (\omega/\omega_{ip})^{\psi_i}]. \quad (16)$$

Let us term Eq. (8) the third generalized Jonscher equation, the GJ3, and, when symmetric conditions apply as in Eq. (16), the generalized Fuoss-Kirkwood-Jonscher equation (GFKJ). As I shall show elsewhere (work in progress), the

ZC and the GFKJ can yield remarkably similar results when the ψ_i of the ZC and the ψ_i of the GFKJ are taken to be different but connected by a simple relation. This connection reduces the need for a complete I_i function for the GFKJ.

THE DISTRIBUTION OF ACTIVATION ENERGIES MODEL

The DAE model, which will be expressed in terms of an I_i which may be applied at either the $i = Z$ or the $i = \epsilon$ level, is based on an exponential distribution of activation energies E . The probability density function for E which will be used here may be written as

$$F_i(E) = \begin{cases} 0 & E < E_{i0}, \\ N_i e^{-N_i E} & E_{i0} \leq E \leq E_{i1}, \\ N_i e^{(\eta_{i2} - \eta_{i1})E_i - \eta_{i2} E} & E_{i1} \leq E \leq E_{i\infty}, \\ 0 & E > E_{i\infty}, \end{cases} \quad (17)$$

where N_i is a normalization constant, η_{i1} and η_{i2} are temperature-independent constants, and the smallest and largest activation energies are E_{i0} and $E_{i\infty}$, with¹² $E_{i\infty} < \infty$. This probability density has been used in an earlier analysis of transient response of a DAE system¹⁰ and leads to t^{-q} response, with two possibly different values of q , over the midtime range. Let us define $\lambda_{ij} \equiv kT\eta_{ij}$, with $j = 1$ and 2 , and $\mathcal{E} \equiv E/kT$. When $\eta_{i1} = \eta_{i2}$, $F_i(E)$ reduces to simple exponential dependence on E , a model which generally yields¹² asymmetric complex plane curves, such as those predicted by the Davidson-Cole²³ and Williams-Watts²⁴ formulas. The derivation, predictions, and justification of this simpler model have been discussed in detail elsewhere.^{10,12} It may be designated the DAE₁ model as opposed to the present general model, the DAE.

Both models assume that a thermally activated response time τ_i is the product of a possibly thermally activated elemental resistance and a possibly thermally activated elemental capacitance.^{12,25} Thus, we take

$$R_i = R_{ai} e^{\alpha_i \mathcal{E}}, \quad (18)$$

$$C_i = C_{ai} e^{\beta_i \mathcal{E}}, \quad (19)$$

and

$$\tau_i = C_{ai} R_{ai} e^{(\alpha_i + \beta_i) \mathcal{E}} \equiv \tau_{ai} e^{\gamma_i \mathcal{E}}. \quad (20)$$

The quantities with "a" subscripts are taken temperature independent, and α_i and β_i are also temperature independent in the simplest situation. These assumptions lead¹² to the following expression for the general DAE model:

$$I_i = M_i \left(\int_1^{r_1} \frac{W^{\phi_{i1} - 1} dW}{1 + i s W} + r_{i1}^{\phi_{i1} - \phi_{i2}} \int_{r_1}^{r_2} \frac{W^{\phi_{i2} - 1} dW}{1 + i s W} \right), \quad (21)$$

where

$$M_i \equiv \left\{ \phi_{i1}^{-1} (r_{i1}^{\phi_{i1}} - 1) + \phi_{i2}^{-1} r_{i1}^{\phi_{i1}} [(r_{i2}/r_{i1})^{\phi_{i2}} - 1] \right\}^{-1}, \quad (22)$$

and

$$W \equiv \tau_i / \tau_{i0} \equiv \exp[\gamma_i (\mathcal{E} - \mathcal{E}_{i0})].$$

Here

$$r_{i1} \equiv \tau_{i1} / \tau_{i0} = \exp[\gamma_i (\mathcal{E}_{i1} - \mathcal{E}_{i0})], \quad (23)$$

$$r_{i2} \equiv \tau_{i\infty} / \tau_{i0} + \exp[\gamma_i (\mathcal{E}_{i\infty} - \mathcal{E}_{i0})], \quad (24)$$

$$s \equiv \omega \tau_{0i} = \omega \tau_{ai} \exp[\gamma_i \mathcal{E}_{i0}], \quad (25)$$

$$\phi_{\epsilon j} \equiv (\beta_{\epsilon} - \lambda_{\epsilon j}) / \gamma_{\epsilon}, \quad (26)$$

and

$$\phi_{Zj} \equiv (\alpha_Z - \lambda_{Zj}) / \gamma_Z. \quad (27)$$

The quantity s is a normalized frequency variable, and the r_j 's are related to the span of the activation energy distribution. The integrals can be expressed in terms of the hypergeometric function for arbitrary ϕ_{ij} values, and closed forms may be written for integer and many fractional values.¹² Unlike the ψ_{ij} of Eq. (8), which fall in the range $0 < \psi_{ij} < 1$, the ϕ_{ij} may have arbitrary positive and negative values so long as $E_{i\infty} < \infty$.

For convenience from now on, we shall usually suppress the i subscript, with the understanding that all results shown apply for either the $i = \epsilon$ or the $i = Z$ situations. The asymmetric DAE₁ simplification¹² of the general DAE expression of Eq. (21) follows when one sets $r_1 = r_2 \equiv r$ and/or $\phi_1 = \phi_2 \equiv \phi$. Another important simplification, the DAE₂, one which yields symmetric results, follows for the choices $r_1 = r_2^{1/2}$ and $\phi_1 = -\phi_2 \equiv \phi$ in Eq. (21). One finds that the peak value of $-I''$ vs $\log(s)$ then occurs at $s = s_p \equiv r_1^{-1}$. The relation $r_1 = r_2^{1/2}$ requires that $E_1 = (E_{\infty} + E_0)/2$, and thus $\omega_p \equiv \tau_p^{-1} = s_p / \tau_0 = \{\tau_a \exp[\gamma(\mathcal{E}_{\infty} + \mathcal{E}_0)/2]\}^{-1}$, the angular frequency at the peak. Symmetric complex plane curves for the DAE₂ for different values of ϕ and r_2 are presented in Fig. 1. The $\phi = 0$ curve is, of course, the same as the $\phi = 0$ result for the DAE₁.¹² Notice that in terms of the gen-

eral normalized admittance I and normalized frequency s , both the DAE₁ and DAE₂ expressions are two-parameter models. In un-normalized form they involve four parameters.

SOME SPECIFIC ϕ TEMPERATURE DEPENDENCIES FOR THE DAE MODEL

The ϕ_1 and ϕ_2 parameters in Eq. (21) determine the effective power-law frequency response exponents in CPE-like regions of the response¹² and are thus very important quantities. Although the previous discussion of general DAE₁ ϕ temperature dependence¹² applies fully to the ϕ 's of the DAE and DAE₂ as well, it is worthwhile discussing some important specializations of the general expressions of Eqs. (26) and (27). To allow a single ϕ equation to represent either $i = \epsilon$ dielectric system response or $i = Z$ conductive system response, take χ equal to either β or α , depending on the situation considered. The DAE₁ condition $\phi_1 = \phi_2 \equiv \phi$ implies that $\eta_1 = \eta_2 \equiv \eta$. Then ϕ for the DAE₁ may be written as

$$\phi_{\text{DAE}_1} = (\chi - kT\eta) / (\alpha + \beta). \quad (28)$$

Even when α and/or β are temperature dependent,¹² ϕ will decrease with increasing T for the usual $\eta > 0$ situation. The $T \rightarrow 0$ intercept may differ, however, between the $i = \epsilon$ and $i = Z$ cases since although we expect $\alpha > 0$, we may have $\beta < 0$. Note that when $\alpha = \beta = 0$, the system is not thermally activated and ω_p is temperature independent. Although $\eta = 0$ in this case, the ratios $\alpha/(\alpha + \beta)$ and $\beta/(\alpha + \beta)$ need not necessarily be zero, so ϕ may have a finite value. The results may then be taken to apply to a situation where τ is not thermally activated but may still be distributed. This is not the same, of course, as a thermally activated situation with $\phi = 0$.

Next consider the DAE₂ condition $\phi_1 = -\phi_2 \equiv \phi$. This leads to $2\chi = kT(\eta_1 + \eta_2)$. Since η_1 and η_2 are temperature independent and χ cannot be directly proportional to temperature,¹² one requires $\eta_2 = -\eta_1 \equiv \eta$, a result which yields a symmetric, peaked probability density for E when $\eta > 0$. Thus one obtains

$$\phi_{\text{DAE}_2} = (\chi + kT\eta) / (\alpha + \beta), \quad (29)$$

which increases with temperature for $\eta > 0$.

The temperature dependencies shown in Eqs. (28) and (29) are linear when α and β are temperature independent. Let us consider one further degree of complexity, however, and assume that the preexponential factor and the activation energy of the relaxation time are linearly related.¹² Then $\chi = \chi_0[1 - T/T_0]$, where χ_0 is temperature independent. For simplicity let us consider a dielectric system with $\beta = 0$. Then one finds from Eq. (29)

$$\phi_{\epsilon} = [(\alpha_0/\eta)(T^{-1} - T_0^{-1})]^{-1}; \quad (30)$$

thus ϕ_{ϵ}^{-1} is proportional to T^{-1} .

It is often found⁶⁻⁸ that a thermally activated system nevertheless exhibits power-law exponents independent of temperature. This possibility follows from Eqs. (28) and (29) if $\eta = 0$ or if $|kT\eta| \ll |\chi|$ over the range of temperatures considered and α and β are temperature independent. Alternati-

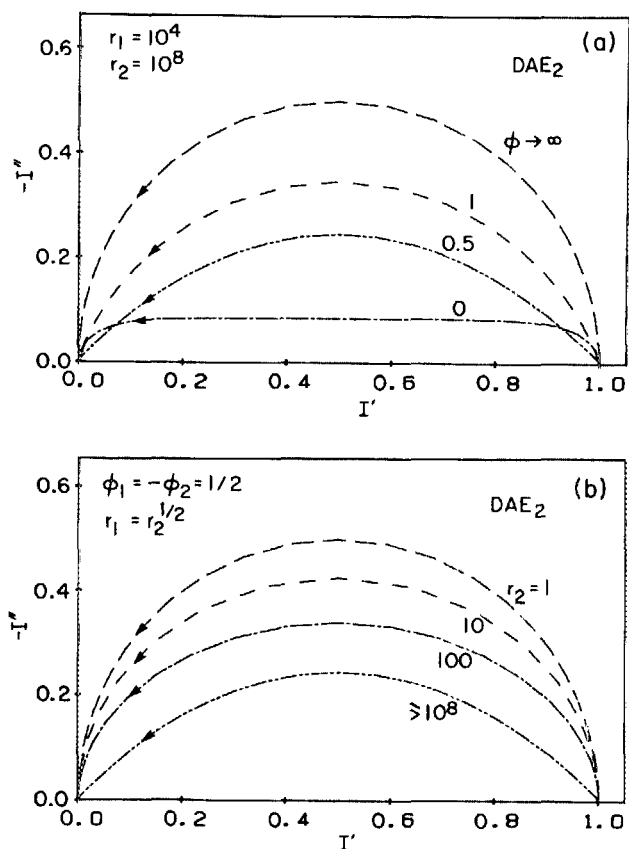


FIG. 1. DAE₂ complex plane response for symmetrical situations. (a) r_1 and r_2 fixed and $\phi \equiv \phi_1 = -\phi_2$ variable ($\phi \rightarrow \infty$ is Debye response), and (b) $\phi = 0.5$ and r_2 and $r_1 = \sqrt{r_2}$ variable ($r_1 \rightarrow 1$ yields Debye response).

vely, one often observes for conductive systems that the exponents decrease with increasing temperature^{16,26} as in Eq. (28). Finally, when the exponents for dielectric systems are found to be temperature dependent they usually increase with temperature,^{6-8,27,28} and their temperature dependence seems to be consistent with that of Eqs. (29) or (30).

COMPARISON OF VARIOUS MODEL PREDICTIONS

In order to allow plotting of the various equations considered herein versus the single normalized frequency s , it is convenient to use the present $s \equiv \omega\tau_0$, which involves the smallest relaxation time of the system for the DAE, and take $s = \omega$ for the UDR equations, their generalizations, and the ZC. These choices ensure that peak positions of $\log_{10}(-I'')$ vs $\log_{10}(s)$ will match for the symmetrical curves.

When $\phi_1 = -\phi_2 \equiv \phi > 0$ and $r_1 = \sqrt{r_2}$, the DAE₂ $\log(-I'')$ vs $\log(s)$ curve is entirely symmetric around its peak at $s_p r_1 = 1$. Then for large r_2 values I_{DAE_2} involves only the parameters ϕ and ω_p (or τ_p), similar to the $\psi_3 = \psi_4 \equiv \psi$ and ω_p parameters of the GFKJ form of Eq. (8) in the general symmetric case. Figure 2 shows a comparison of I'' predictions for the DAE₂ with $r_1 = 10^4$, and $\phi = 0.5$; the GFKJ with $\tau_p = 10^4$ and $\psi = 0.5$; the ZC with $\tau_c = 10^4$ and $\psi = 0.5$; and the Debye model. We see that the ZC agrees appreciably less well with the other two broad-spectrum models; the DAE₂ and the GFKJ are remarkably similar for $r_2^{-1} < s < 1$; and the DAE₂ shows the physically necessary $\omega^{\pm 1}$ dropoff for $s < r_2^{-1}$ and $s > 1$ or, equivalently, for $\omega < \tau_0^{-1}$ and $\omega > \tau_0^{-1}$.

Also of interest is comparison in the complex plane of the full three I predictions and Debye response. This is shown in Fig. 3, and again the DAE₂ and GFKJ results are remarkably close to each other and the ZC is appreciably different. Here the arrows indicate the direction of increas-

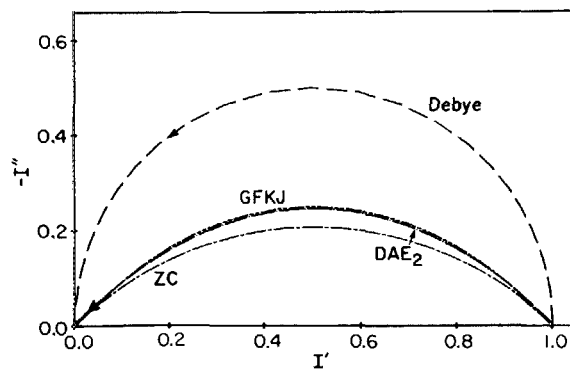


FIG. 3. Complex plane plot for Debye, GFKJ, DAE₂, and ZC situations. Same parameter choices as in Fig. 2.

ing frequency and the DAE₂ $\omega^{\pm 1}$ regions do not show and would only do so for a much smaller value of r_2 . For $\phi > 0$ the shape of the DAE₂ complex plane arc stabilizes for large r_2 and only its frequency scale changes with increasing r_2 , with the peak of $-I''$ as $s = s_p = r_1^{-1}$. Thus the curve for $r_2 = 10^4$ is very close in shape to that shown for $r_2 = 10^8$, and there is negligible difference in shape between $r_2 = 10^8$ and $r_2 = 10^{12}$ curves. Note that even for $r_2 = 10^{12}$, when $\gamma \equiv \alpha + \beta = 1$ the quantity $(E_\infty - E_0)$ is less than $30 kT$, not an extremely wide activation energy span.

The results of Fig. 4 show that the general DAE and the I'' of Eq. (8), the GJ3 equation, also yield excellent agreement for nonsymmetrical peaked curves. Since no expression for I' associated with the I'' of Eq. (8) is available in the unsymmetrical case, we have adjusted the parameters of the Jonscher curve so that it agrees exactly at one point with the DAE₂ prediction. Note that the slope of the $\log(-I'')$ vs $\log(s)$ DAE₂ curve is $-\phi_2 > 0$ for $r_2^{-1} < s < r_1^{-1}$ and $-\phi_1 < 0$ for $r_1^{-1} < s < 1$. Agreement between the two mod-

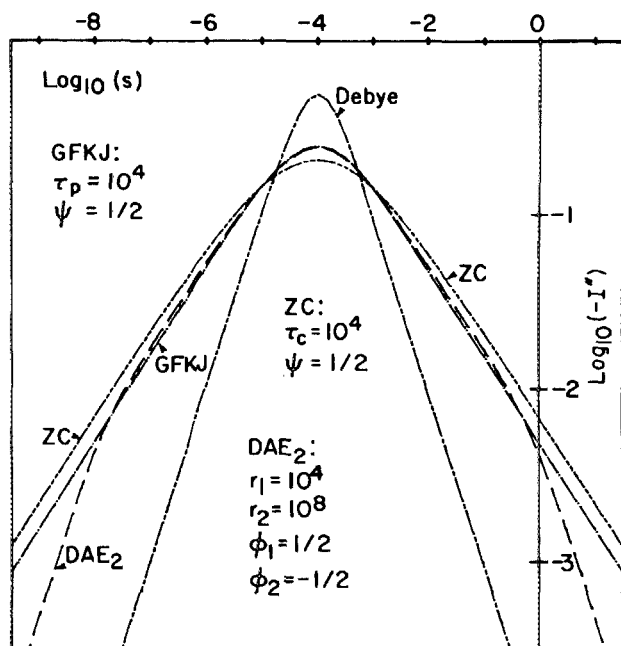


FIG. 2. Comparison of Debye, GFKJ, DAE₂, and ZC predictions of $\log(-I'')$ vs $\log(s)$ for the parameter choices shown.

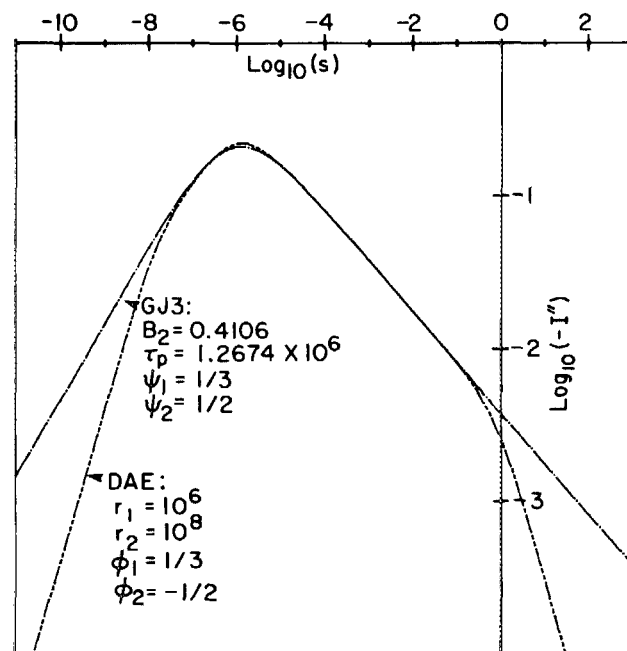


FIG. 4. $\log(-I'')$ vs $\log(s)$ curves for unsymmetrical GJ3 and DAE equation situations.

els would extend over a wider frequency range if r_2 and r_1 were taken larger so the $\omega^{\pm 1}$ regions didn't appear within the range considered.

Finally, Fig. 5 shows three-dimensional perspective plotting²⁹ results for the situation where ϕ_1 and ϕ_2 are both positive, a condition often found for conducting systems. We have used 3D plotting here because it is important to illustrate the frequency response of the real and imaginary parts of I simultaneously. In order to show response over a wide

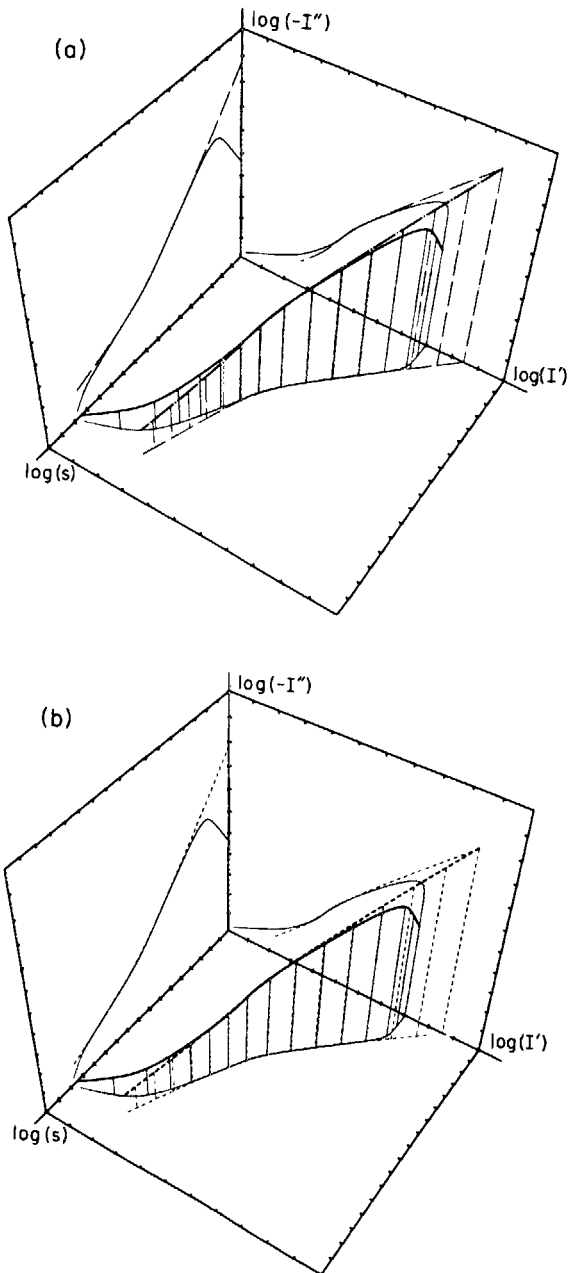


FIG. 5. Logarithmic three-dimensional perspective plots and their projection curves for the DAE with $\phi_1 > 0$ and $\phi_2 > 0$ and for two GJ2 curves fit to the DAE results: (a) I'' fit for GJ2 (dash-dot line); (b) full I fit for GJ2 (dashed line). For the DAE (solid lines): $r_1 = 10^6$, $r_2 = 10^{12}$, $\phi_1 = 1/3$, $\phi_2 = 2/3$. Parameter estimates: GJ2 I'' fit: $B_1 = (2.901 \pm 0.418) \times 10^{-4}$, $\tau_c = (7.411 \pm 2.233) \times 10^4$, $\psi_1 = (0.2201 \pm 0.0189)$, and $\psi_2 = (0.6856 \pm 0.0079)$. GJ2 I fit: $B_1 = (4.603 \pm 0.700) \times 10^{-5}$, $\tau_c = (1.836 \pm 0.548) \times 10^5$, $\psi_1 = (0.2933 \pm 0.0089)$, and $\psi_2 = (0.7067 \pm 0.0089)$.

range, we have plotted $\log(-I'')$, $\log(I')$, and $\log(s)$ here. Thus one of the projections is just the ordinary $\log(-I'')$ vs $\log(s)$ plot and another is the log complex plane plot. The tick marks in these plots are spaced at unity intervals (factor of 10), and the origin of $[\log(-I''), \log(I'), \log(s)]$ is at $(-8, -7, -14)$. The solid curve is that for the general DAE with the values listed in the caption. Note that it shows a low-frequency peak. Also shown for comparison are two GJ2 curves which do not have peaks. Separate plots are presented for added clarity. The GJ2 curve of Fig. 5(a) was obtained by fitting only I'' DAE results with the GJ2 formula, using weighted nonlinear least squares. Notice that its predicted I' results are rather poor, particularly at the high-frequency end. The curve of Fig. 5(b) was obtained by using weighted CNLS to fit the DAE complex "data" with the full GJ2 I equation. In both of these fits only DAE "data" satisfying $10^{-9} \leq s \leq 10^{-3}$ were used in order to avoid the $s^{\pm 1}$ regions of the DAE at the frequency extremes. Note that the CNLS fitting results show that for the present case the GJ2 can well simulate the DAE over a wide frequency region and, of course, *vice versa*. But the estimated parameter results given in the caption also show that conventional fitting of the imaginary part only is less satisfactory, as far as yielding good results for the real part and for parameter predictions, than is CNLS fitting. Finally, the first form of Eq. (10), without the GJ2 specializations, was also fit to the DAE "data." Exactly the same fit was found as with the GJ2, as expected, since both equations had four free parameters. But the relative standard deviations of the parameters were smaller with the first form of Eq. (10) than with the GJ2, and the parameter correlations were far smaller. In fact, all but one of those for the GJ2 exceeded 0.9! These results suggest that CNLS fitting is better than imaginary part fitting and that the general Eq. (10) result is more appropriate, at least in this instance, than its Jonscher specialization.

The above results show that the DAE model is capable of fitting all the "UDR" equations and their generalizations extremely well. In addition, it has been found (Ref. 30 and work in progress) that the DAE can fit very well the predictions of virtually all other models which have been used in the past to analyze dielectric or conductive system data. Such fitting, carried out by CNLS over a wide frequency range, generally yields somewhat different values of the DAE ϕ 's and the ψ exponents of the other models, as is, in fact, required since the ϕ 's and ψ 's have different ranges. Nevertheless, the fitting agreement allows one to determine relations between the ϕ 's and the ψ 's of the other equations. Such relations may then be employed, along with the temperature dependence of a given ϕ , to predict the possible temperature dependence of a ψ directly determined from data fitting using an equation like the ZC or the GFKJ.

DISCUSSION

The DAE model, Eq. (21) and its simplifications, yields frequency response results at either the impedance or the complex dielectric constant level which can accurately simulate the response of the ZC, the Davidson-Cole, the Williams-Watts, and all three of the UDR equations. Thus it should be able to fit quite well all the vast amount of experi-

mental data which these equations have been used in the past to represent. Further, unlike these equations, the DAE model is less empirical. The DAE is a model which falls between macroscopic models/empirical equations and microscopic models, models which have the potential for greater accuracy and for yielding expressions for all parameters which involve only basic microscopic material properties. But since accurate microscopic modeling of even small-signal frequency response involves the solution of a many-body problem with appreciable short- and possibly long-range coupling, no adequate, fully microscopic solution is yet available. Further, since the interacting entities may be ions, charged defects, electrons, holes, dipoles, or combinations thereof, several different microscopic theories for different situations will certainly be required to yield response like the single DAE model.

The main somewhat empirical element in the DAE model is the use of an activation energy probability density distribution which depends exponentially on E . This choice is a very natural one and is somewhat justified elsewhere.^{10,12} Further, several statistically based approaches to obtaining an activation energy exponential probability density were discussed at the March 1985 APS meeting and should appear in the literature in due course. (See especially Ref. 37 and references therein.) When any microscopic theory yields an expression for η , the strength of the exponential distribution, in terms of basic microscopic parameters, the result may be directly incorporated into the DAE, removing an empirical element, at least for the particular microscopic situation considered.

It is worth emphasizing that the exponential probability density distribution $F(E)$ for activation energies, on which the entire DAE approach is based, is directly related^{10,12} to a finite-range Pareto distribution for τ , one with $\mathcal{G}(\tau) \propto \tau^{-n}$ for a finite range of τ . Now Shockley³¹ and Montroll and Shlesinger³² have shown that a multiplicative picture, where overall success depends on the success of many independent subtasks, can lead to a log-normal distribution $\mathcal{G}(x)$ of a variable x . Further, Montroll and Shlesinger have shown that this distribution is well mimicked by a reciprocal distribution when the dispersion of the overall process is large, and by a Pareto distribution when an inherent amplification process is present. The probability density $\mathcal{G}(x)$ in the last case is interpreted as the distribution function of a divergent branching process in which the mean value of $\mathcal{G}(x)$ is infinite.³²

Let us apply these results to the present DAE model, remembering that it involves finite-range rather than infinite-range distributions in order to achieve the physical realizability eschewed by many infinite-range models. Let such a finite range be understood in the following. Thus problems with infinite first and higher moments do not arise. We may identify the multiplicative process with relaxation, so $x = \tau$. Then when τ exhibits a (truncated) log-normal distribution and is thermally activated, E will have a (truncated) normal distribution. The natural interpretation is that thermal activation response is then the result of many independent additive processes (ones with different activation energies) distributed with an overall (truncated) normal probability

density. Alternatively when $\mathcal{G}(\tau)$ is well approximated by a τ^{-1} or τ^{-n} probability density, $F(E)$ is distributed exponentially, as in the present DAE model. In this case the original Gaussian density has been replaced by an exponential waiting-time distribution. The presence of the amplification process in the Pareto (or exponential) distribution possibly may allow the overall response to be interpreted as involving many dependent, coupled elemental processes. There is clearly a need for microscopic modelling here. Finally, it should be emphasized that small-signal ac response is only sensitive to the overall general shape of a probability distribution density, not to the fine details of the distribution.³³

Most earlier DAE studies have already been discussed,¹² but it is worth mentioning that of Bernasconi *et al.*³⁴ which shares a few common features with the DAE model, including the DAE₁ exponential activation energy probability density choice (but taken untruncated). Only results for the low-frequency limit have been presented by these authors and are of simple CPE form, however. Ngai and White³⁵ have obtained CPE response arising from the presence of ubiquitous correlated states associated with many-body interactions in condensed matter. It is not unreasonable to expect the energy of these states to be distributed with exponential probability density, as in the present DAE model. All real systems, even single crystals, show some disorder at finite temperatures, and it is likely that this disorder leads to a distribution of activation energies for, e.g., dipole rotation or ionic hopping.

A somewhat different approach has been recently described by Dissado and Hill.³⁶ Like the DAE model, it is intermediate between a macro and a micro approach, but it envisages the presence of many clusters with intra and inter-cluster interactions. Its solution also yields response in the form of a hypergeometric function as well as good agreement with some data of the type well described by the second and third UDR equations, Eqs. (2) and (3). But it involves the $\psi_{\epsilon_3} = m$ and $\psi_{\epsilon_4} = 1 - n$ Jonscher power-law exponents, which are limited to the range (0,1); no limiting $\omega^{\pm 1}$ responses are shown; it does not yield explicit expressions for the temperature dependencies of the power-law exponents; and its range of applicability may be only for very low temperatures.

Because of the importance and usefulness of both weighted CNLS and the present DAE model, this model has been incorporated as a general circuit element in a very flexible equivalent circuit which is part of a powerful CNLS computer program available from the author. The complete circuit also includes the ZC, the Davidson-Cole, Williams-Watts, CPE, and GJ2 equations as possible fitting elements.

ACKNOWLEDGMENTS

I much appreciate the helpful comments of Robert L. Hurt and Stephen W. Kenkel and the support of the work by the U.S. Army Research Office.

¹A. K. Jonscher, *Nature* **250**, 191 (1974); **253**, 717 (1975); **256**, 566 (1975).

²H. Fricke, *Philos. Mag.* **14**, 310 (1932).

³K. S. Cole and R. H. Cole, *J. Chem. Phys.* **9**, 341 (1941).

⁴J. R. Macdonald, *Solid State Ion.* **13**, 147 (1984).

⁵A. K. Jonscher, *Colloid Polym. Sci.* **253**, 231 (1975).

⁶A. K. Jonscher, *The Universal Dielectric Response: A Review of Data and*

their New Interpretation (Chelsea Dielectrics Group, Chelsea College, University of London, 1978), pp. 27 and 29.

⁷A. K. Jonscher, *Phys. Thin Films* **11**, 202 (1980).

⁸A. K. Jonscher, *Dielectric Relaxation in Solids* (Chelsea Dielectrics, London, 1983).

⁹J. R. Macdonald and M. K. Brachman, *Rev. Mod. Phys.* **28**, 393 (1956).

¹⁰J. R. Macdonald, *J. Appl. Phys.* **34**, 538 (1963).

¹¹R. Syed, D. L. Gavin, C. T. Moynihan, and A. V. Lesikar, *J. Am. Ceram. Soc.* **64**, C118 (1981).

¹²J. R. Macdonald, *J. Appl. Phys.* **58**, 1955 (1985).

¹³J. R. Macdonald, J. Schoonman, and A. P. Lehn, *J. Electroanal. Chem.* **131**, 77 (1982).

¹⁴D. P. Almond and A. R. West, *J. Electroanal. Chem.* **186**, 17 (1985).

¹⁵A. K. Jonscher and J.-M. Réau, *J. Mater. Sci.* **13**, 563 (1978).

¹⁶J. R. Macdonald and G. B. Cook, *J. Electroanal. Chem.* **168**, 335 (1984). Further related work on Na β -alumina by Macdonald and Cook has been accepted for publication by *J. Electroanal. Chem.*

¹⁷D. P. Almond, A. R. West, and R. J. Grant, *Solid State Commun.* **44**, 1277 (1982).

¹⁸J. R. Macdonald, *Solid State Ion.* **15**, 159 (1985).

¹⁹D. Ravaine and J.-L. Souquet, *C. R. Acad. Sci. Ser. C* **277**, 489 (1973).

²⁰R. M. Fuoss and J. G. Kirkwood, *J. Am. Chem. Soc.* **63**, 385 (1941).

²¹J. R. Macdonald, *J. Chem. Phys.* **20**, 1107 (1952). The term $[1 + 0.5 \exp(-2x)]$ in the denominator of Eq. (10) of this work should be raised to the second power.

²²R. Lovell, *J. Phys. C* **7**, 4378 (1974).

²³D. W. Davidson and R. H. Cole, *J. Chem. Phys.* **19**, 1484 (1951).

²⁴G. Williams and D. C. Watts, *Trans. Faraday Soc.* **66**, 80 (1970).

²⁵J. F. McCann and S. P. S. Badwal, *J. Electrochem. Soc.* **129**, 551 (1982).

²⁶H. Engstrom, J. B. Bates, and J. C. Wang, *Solid State Commun.* **35**, 543 (1980).

²⁷N. O. Birge, Y. H. Jeong, S. R. Nagel, S. Bhattacharya, and S. Susman, *Phys. Rev. B* **30**, 2306 (1984).

²⁸N. Alberding, R. H. Austin, S. S. Chan, L. Eisenstein, H. Frauenfelder, I. C. Gunsalus, and T. M. Nordlund, *J. Chem. Phys.* **65**, 4701 (1976).

²⁹J. R. Macdonald, J. Schoonman, and A. P. Lehn, *Solid State Ion.* **5**, 137 (1981).

³⁰J. R. Macdonald, *Bull. Am. Phys. Soc.* **30**, 587 (1985).

³¹W. Shockley, *Proc. IRE* **45**, 279 (1957).

³²E. W. Montroll, and M. F. Shlesinger, *Proc. Natl. Acad. Sci. USA* **79**, 3380 (1982).

³³C. J. F. Böttcher, and P. Bordewijk, *Theory of Electrical Polarization*, Vol. II (Elsevier, Amsterdam, 1978), pp. 47-48.

³⁴J. Bernasconi, H. U. Beyeler, S. Strässler, and S. Alexander, *Phys. Rev. Lett.* **42**, 819 (1979).

³⁵K. L. Ngai and C. T. White, *Phys. Rev. B* **20**, 2475 (1979). See also K. L. Ngai, *Comm. Solid State Phys.* **9**, 127 (1979), 141 (1980).

³⁶L. A. Dissado and R. M. Hill, *Proc. R. Soc. London Ser. A* **390**, 131 (1983); *J. C. S. Faraday* **80**, 291 (1984).

³⁷J. R. Macdonald (unpublished).